Coupled Tensor Decompositions for Hyperspectral Super Resolution

David Brie
CRAN UMR 7039 - Université de Lorraine - CNRS

Workshop on Tensor Theory and Methods
Paris, November 23-24, 2022

Outline

Team : CRAN - BioSIS - SiMul

- 1 Pr, 2 Associate Pr., 3 CR, 1 post-doc, 4 PhD students, 1 Engineer
- Analysis and processing of Multidimensional Signals
- Sparse approximation, Matrix and Tensor decompositions, SLRA, Data Fusion, Polarimetric phase retrieval, quaternion signal processing
- Microscopy, Hyperspectral Image Processing, Flow cytometry
- `https://cran-simul.github.io`

Team : CRAN - BioSIS - SiMul

- 1 Pr, 2 Associate Pr., 3 CR, 1 post-doc, 4 PhD students, 1 Engineer
- Analysis and processing of Multidimensional Signals
- Sparse approximation, Matrix and Tensor decompositions, SLRA, Data Fusion, Polarimetric phase retrieval, quaternion signal processing
- Microscopy, Hyperspectral Image Processing, Flow cytometry
- `https://cran-simul.github.io`

Collaborators associated to this work

- Clémence Prévost, Ricardo Borsoi, Konstantin Usevich
  Martin Haardt, Eric Chaumette, José Bermudez, Cédric Richard, Pierre Comon

Introduction

Data fusion

Multimodality = multiple datasets

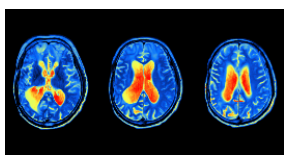

fMRI

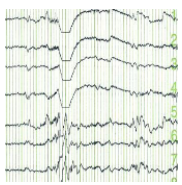

EEG

Brain activity

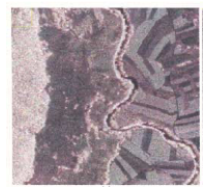

Hyperspectral

Multispectral

Airborne scene

Hyperspectral super-resolution ...

FROM

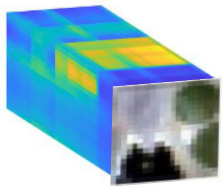

Hyperspectral image

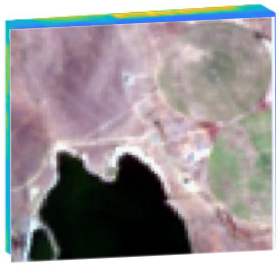

Multispectral image

RECOVER

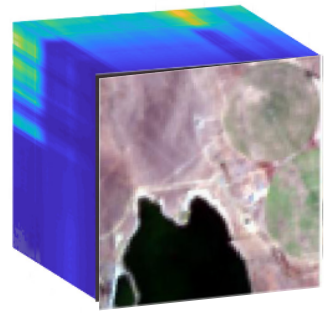

Super-resolution image (SRI)

- ✓ High spatial resolution;
- ✓ High spectral resolution;

... Using low-rank tensor models

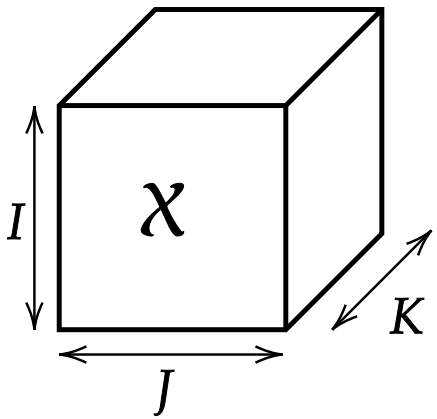

Tensor : array of p dimensions ($p \geq 3$).

Structure-preserving low-rank model for high-dimensional data ;

Uniqueness of Low-rank tensor decompositions.

Tensor observation model

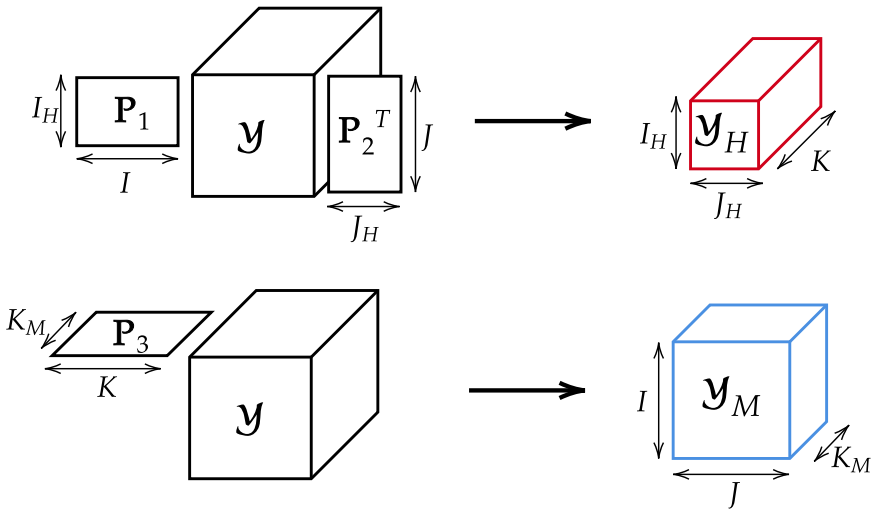

$$\begin{cases} \mathcal{Y}_H &= \mathcal{Y} \bullet_1 \mathbf{P}_1 \bullet_2 \mathbf{P}_2 + \mathcal{E}_H, \\ \mathcal{Y}_M &= \mathcal{Y} \bullet_3 \mathbf{P}_3 + \mathcal{E}_M. \end{cases}$$

- $\mathbf{P}_1$, $\mathbf{P}_2$: Gaussian blurring + downsampling (Wald et al., 1997) ;
- $\mathbf{P}_3$: spectral response function.

Optimization problem

$$\underset{\text{low-rank } \mathcal{Y}}{\text{minimize}} \left\| \mathcal{Y}_H - \mathcal{Y} \underset{1}{\bullet} \mathbf{P}_1 \underset{2}{\bullet} \mathbf{P}_2 \right\|_F^2 + \lambda \left\| \mathcal{Y}_M - \mathcal{Y} \underset{3}{\bullet} \mathbf{P}_3 \right\|_F^2.$$

Low-rank tensor decompositions

- Canonical polyadic decomposition :

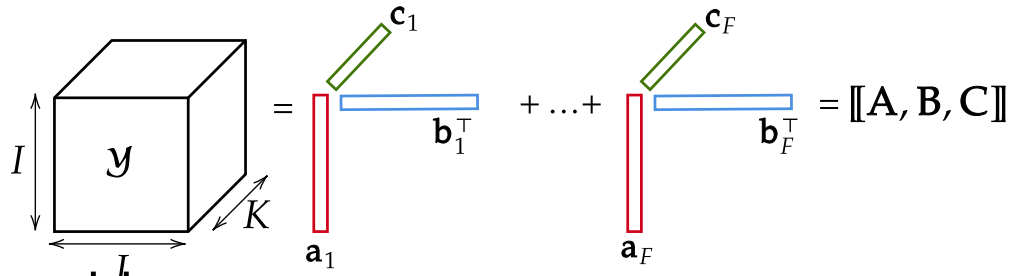

- Tucker decomposition :

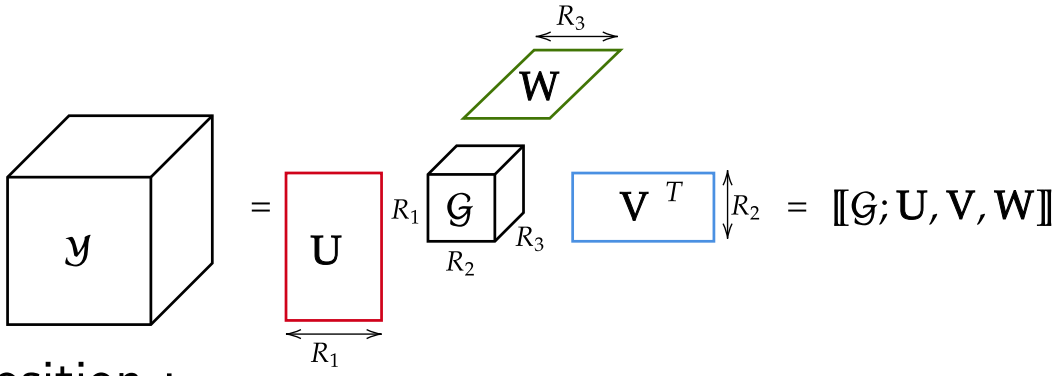

- $LL1$ decomposition :

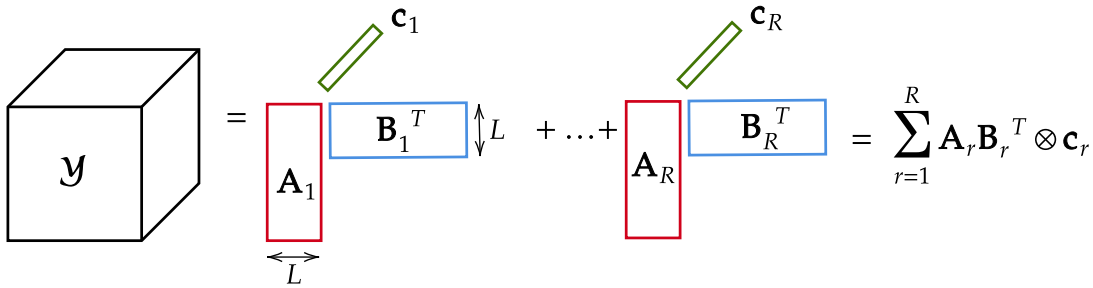

Regularisation via low-rank models

Aim

Recover IJK entries from $IJK_M + I_H J_H K$ observations .

$IJK > IJK_M + I_H J_H K$: Ill-Posed inverse problem

Matrix	**LL1-BTD**	**CPD**	**Tucker**
$(IJ+K-R)R$	$((I+J-L)L+(K-1))R$	$(I+J+K-2)N$	$IR_1+JR_2+KR_3+\prod_{i=1}^{3} R_i - \sum_{i=1}^{3} R_i^2$

- $I = J = K = 100,\ I_H = J_H = 50,\ K_M = 10$;
- $N = LR,\ R_1 = R_2 = LR,\ R_3 = R.$

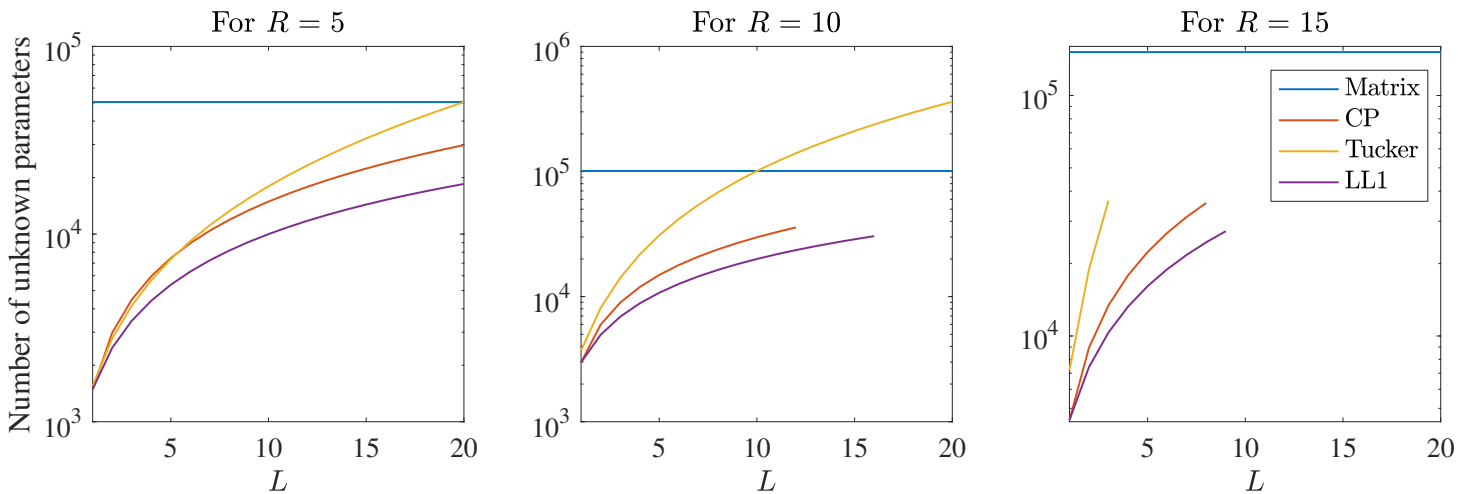

Variations on the model

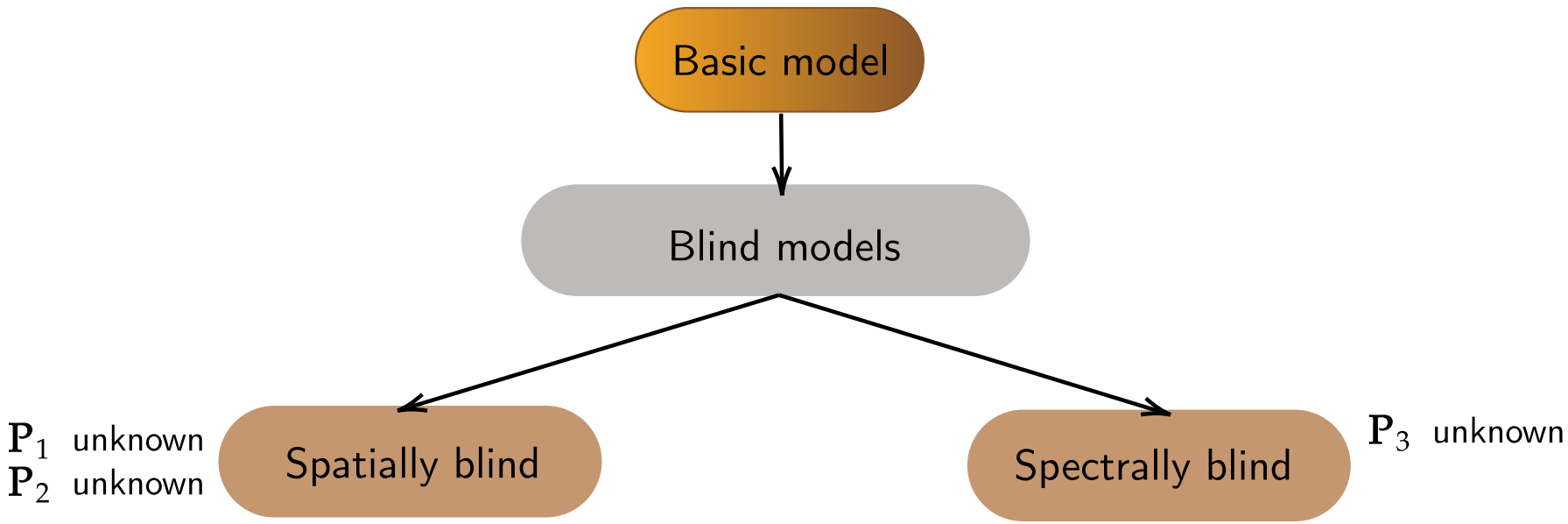

Variations on the model

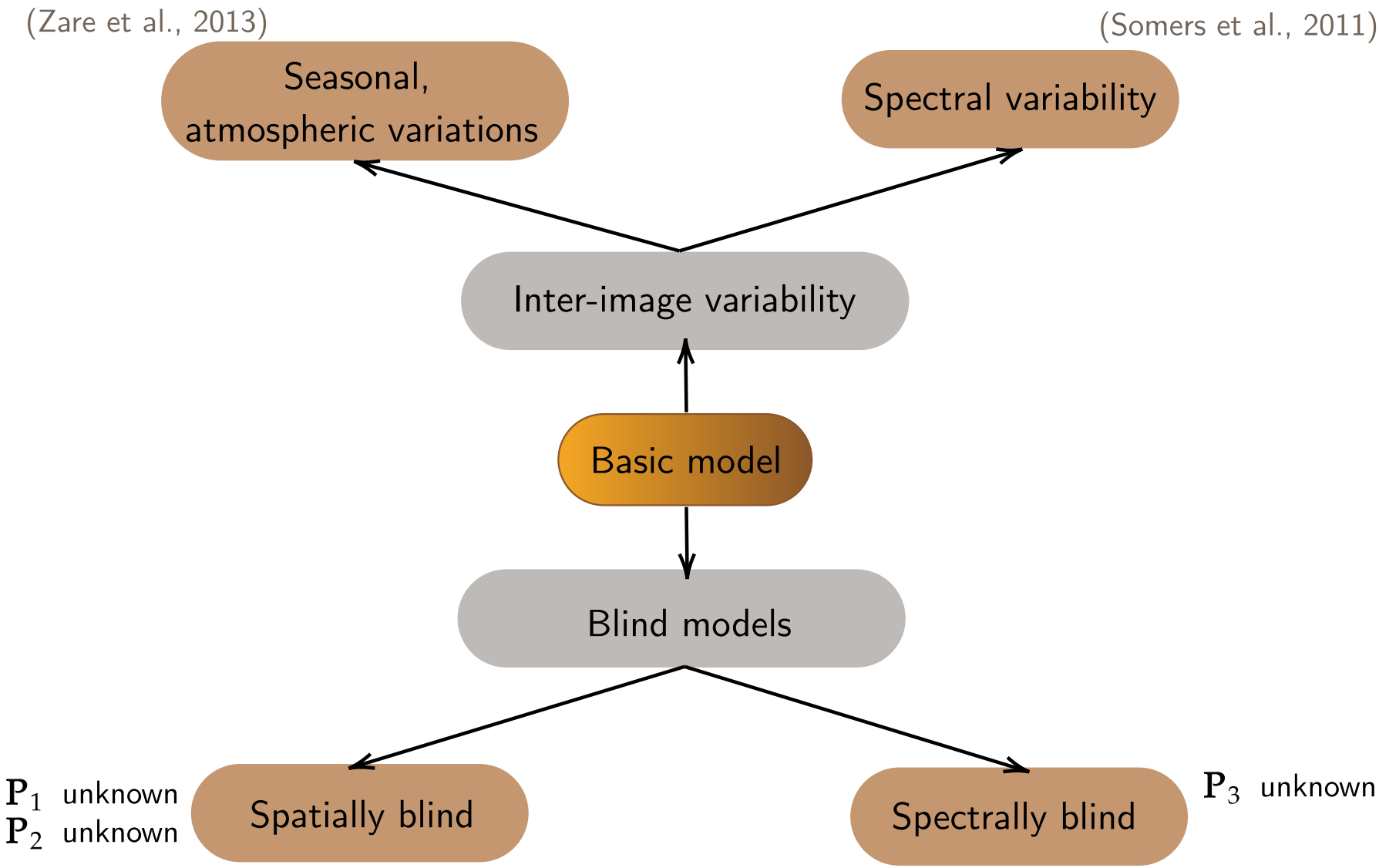

A brief tour of tensor-based HSR

	CPD	**Tucker**	**BTD**
Basic model	(Kanatsoulis, 2018)	(Prévost, 2020)	(Zhang, 2019) (Ding, 2020) (Prévost, 2021)
Blind model	(Kanatsoulis, 2018)	(Prévost, 2020)	(Ding, 2020)
Non-negativity			(Zhang, 2019) (Ding, 2020) (Prévost, 2021)
Variability		(Borsoi, 2021)	(Prévost, 2021)
Performance analysis	(Prévost, 2022)		(PrévostPhD, 2021)

CPD-based HSR

CP approach

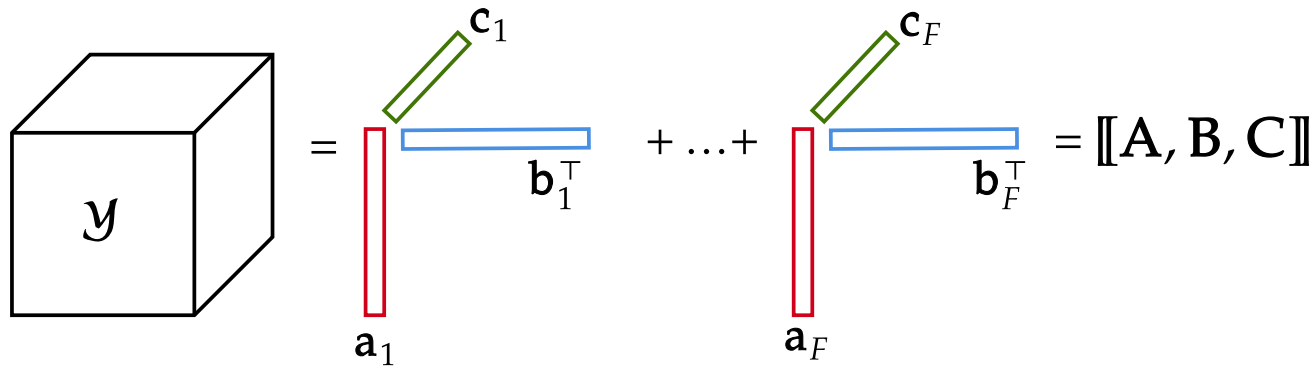

Fully coupled CP model

$$\underset{\widehat{\mathbf{A}},\widehat{\mathbf{B}},\widehat{\mathbf{C}}}{\text{minimize}} \ \left\| \mathcal{Y}_H - [[\mathbf{P}_1\widehat{\mathbf{A}}, \mathbf{P}_2\widehat{\mathbf{B}}, \widehat{\mathbf{C}}]] \right\|_F^2 + \lambda \left\| \mathcal{Y}_M - [[\widehat{\mathbf{A}}, \widehat{\mathbf{B}}, \mathbf{P}_3\widehat{\mathbf{C}}]] \right\|_F^2.$$

Exact generic recovery

$$N \leq \min\{2^{\lfloor \log_2(K_M J) \rfloor - 2}, I_H J_H\}.$$

- Only the identiability of the CPD of $\mathcal{Y}_M$ is required

STEREO : an ALS algorithm

Until *stopping criterion* is met,

1. $\widehat{\mathbf{A}} = \underset{\mathbf{A}}{\operatorname{argmin}}\, \mathbf{f_{CP}}(\mathbf{A}, \widehat{\mathbf{B}}, \widehat{\mathbf{C}})$,
2. $\widehat{\mathbf{B}} = \underset{\mathbf{B}}{\operatorname{argmin}}\, \mathbf{f_{CP}}(\widehat{\mathbf{A}}, \mathbf{B}, \widehat{\mathbf{C}})$,
3. $\widehat{\mathbf{C}} = \underset{\mathbf{C}}{\operatorname{argmin}}\, \mathbf{f_{CP}}(\widehat{\mathbf{A}}, \widehat{\mathbf{B}}, \mathbf{C})$

$\widehat{\mathcal{Y}} = [[\widehat{\mathbf{A}}, \widehat{\mathbf{B}}, \widehat{\mathbf{C}}]]$.

Init : Tenrec (hybrid algorithm)
Updates : (generalized) Sylvester equation

Blind-STEREO

A partially coupled CP model

$$\underset{\substack{\widetilde{\mathbf{A}},\widetilde{\mathbf{B}},\\ \widehat{\mathbf{A}},\widehat{\mathbf{B}},\widehat{\mathbf{C}}}}{\text{minimize}} \quad \|\mathcal{Y}_H - [[\widetilde{\mathbf{A}},\widetilde{\mathbf{B}},\widehat{\mathbf{C}}]]\|_F^2 + \lambda\|\mathcal{Y}_M - [[\widehat{\mathbf{A}},\widehat{\mathbf{B}},\mathbf{P}_3\widehat{\mathbf{C}}]]\|_F^2.$$

Exact recovery

Both the CPD of the HSI and MSI should be unique.

Algorithms

- ALS algorithm, Hybrid algorithm

1. $[[\widehat{\mathbf{A}},\widehat{\mathbf{B}},\widetilde{\mathbf{C}}]] = \text{CPD}(\mathcal{Y}_M)$,
2. $\mathbf{Z} = \text{tSVD}_{R_3}\left(\mathbf{Y}_H^{(3)}\right)$,
3. $\widehat{\mathbf{C}} = \mathbf{Z}(\mathbf{P}_3\mathbf{Z})^{\dagger}\widetilde{\mathbf{C}}$,
4. $\widehat{\mathcal{Y}} = [[\widehat{\mathbf{A}},\widehat{\mathbf{B}},\widehat{\mathbf{C}}]]$.

TD-based HSR

Tucker approach

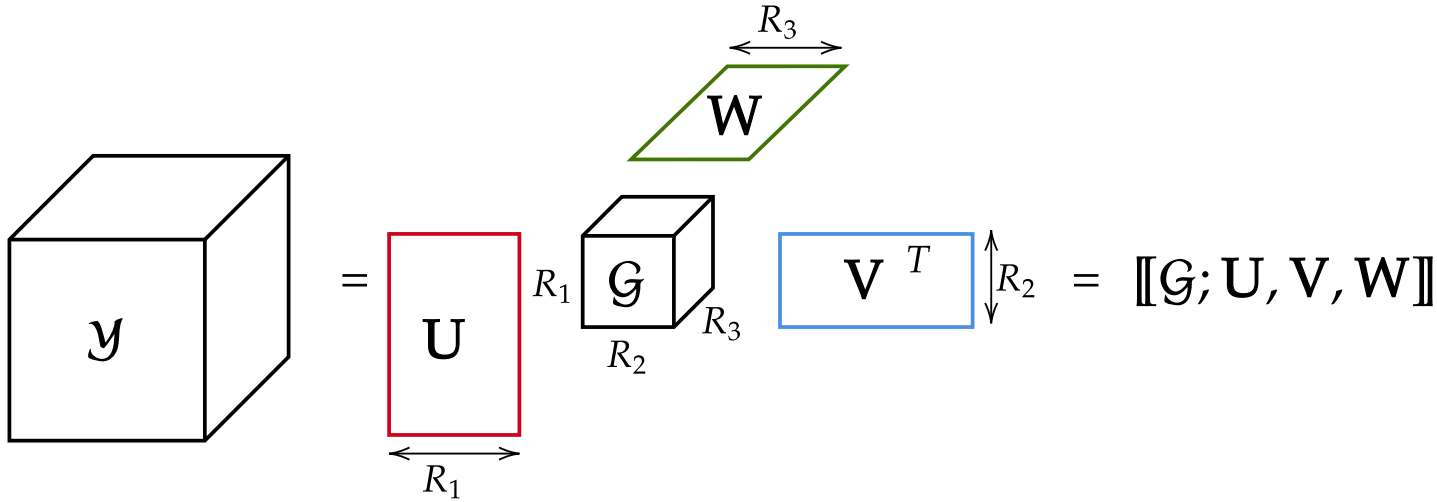

Optimization problem

$$\underset{\widehat{\mathcal{G}},\widehat{\mathbf{U}},\widehat{\mathbf{V}},\widehat{\mathbf{W}}}{\text{minimize}} \ \left\| \mathcal{Y}_H - [[\widehat{\mathcal{G}}; \mathbf{P}_1\widehat{\mathbf{U}}, \mathbf{P}_2\widehat{\mathbf{V}}, \widehat{\mathbf{W}}]] \right\|_F^2 + \lambda \left\| \mathcal{Y}_M - [[\widehat{\mathcal{G}}; \widehat{\mathbf{U}}, \widehat{\mathbf{V}}, \mathbf{P}_3\widehat{\mathbf{W}}]] \right\|_F^2 .$$

SCOTT

- Closed-form algorithms ;
- Exact generic recovery guarantees ;
- Solution to pansharpening.

Exact generic recovery

Assumptions : $\mathbf{P}_1, \mathbf{P}_2, \mathbf{P}_3$ are full-rank ; $\mathcal{G}, \mathbf{U}, \mathbf{V}, \mathbf{W}$ are random ; $R_1 = R_2$, $I_H = J_H$, $I = J$.

1. $\left.\begin{array}{l} R_3 \leq \min(R_1, I_H)^2, \\ a) R_1 \leq I_H \text{ or } b) R_3 \leq K_M, \end{array}\right\} \Rightarrow \widehat{\mathcal{Y}}$ is unique ;
2. $a)$ and $b)$ not satisfied $\Rightarrow$ $\widehat{\mathcal{Y}}$ is not unique.

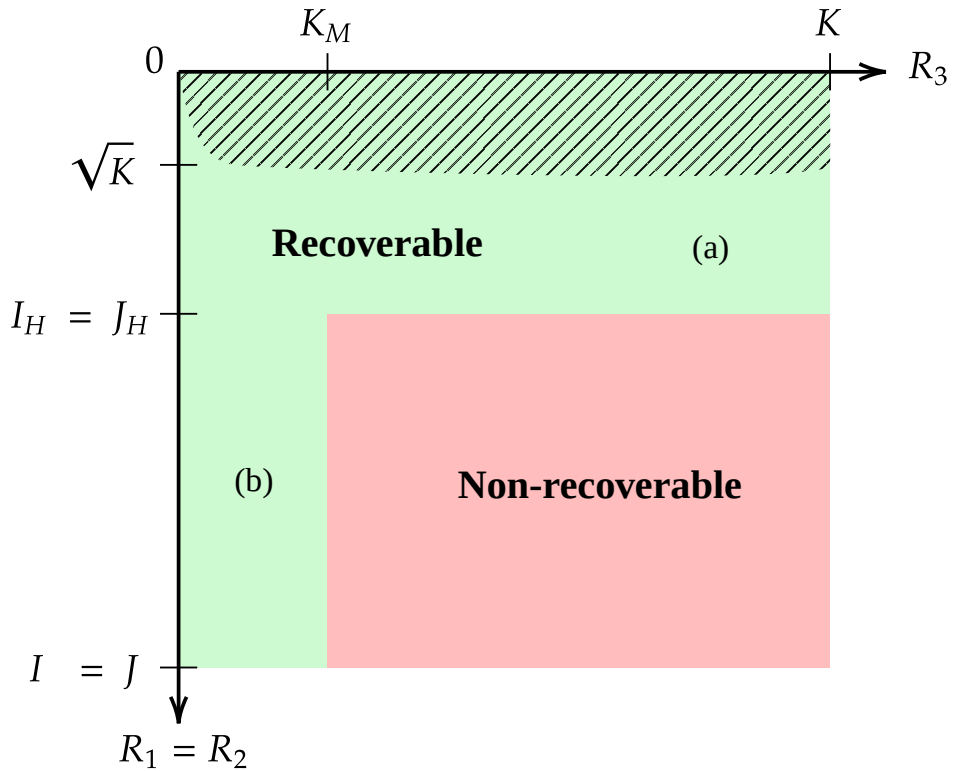

SCOTT : an algebraic approach

1. $\widehat{\mathbf{U}} = \text{tSVD}_{R_1}(\mathbf{Y}_M^{(1)})$, $\widehat{\mathbf{V}} = \text{tSVD}_{R_2}(\mathbf{Y}_M^{(2)})$, $\widehat{\mathbf{W}} = \text{tSVD}_{R_3}(\mathbf{Y}_H^{(3)})$;
2. $\widehat{\mathcal{G}} =$ solve coupled normal equations ;
3. $\widehat{\mathcal{Y}} = [[\widehat{\mathcal{G}}; \widehat{\mathbf{U}}, \widehat{\mathbf{V}}, \widehat{\mathbf{W}}]]$.

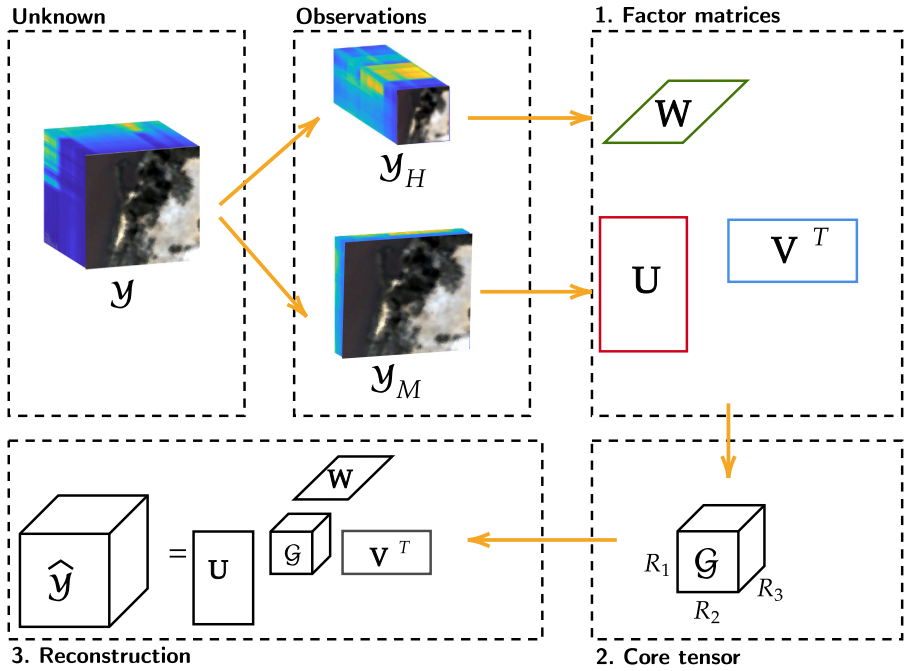

Blind SCOTT (BSCOTT)

Split $\mathcal{Y}_H$, $\mathcal{Y}_M$ into L blocks along the spatial dimensions;

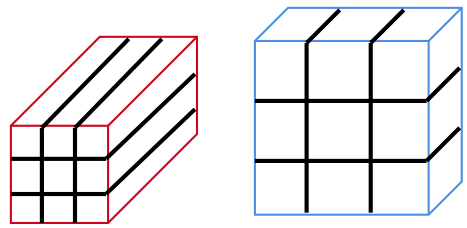

For $\ell \in \{1, \ldots, L\}$, do

1. $\left(\mathcal{Y}_M\right)_\ell \overset{\text{HOSVD}}{\approx} [\![\widehat{\mathcal{G}}_\ell; \widehat{\mathbf{U}}_\ell, \widehat{\mathbf{V}}_\ell, \widetilde{\mathbf{W}}_\ell]\!]$;
2. $\mathbf{Z}_\ell = \text{tSVD}_{R_3}\left(\mathbf{Y}_H^{(3)}\right)_\ell$;
3. $\widehat{\mathbf{W}}_\ell = \mathbf{Z}_\ell \left(\mathbf{P}_3 \mathbf{Z}_\ell\right)^\dagger \widetilde{\mathbf{W}}_\ell$;
4. $\widehat{\mathcal{Y}}_\ell = [\![\widehat{\mathcal{G}}_\ell; \widehat{\mathbf{U}}_\ell, \widehat{\mathbf{V}}_\ell, \widehat{\mathbf{W}}_\ell]\!]$;

End

Experiments

Simulations setup

- Groundtruth SRI $\mathcal{Y}$: satellite-acquired ;
- $\mathbf{P}_3$: Spectral response functions of MS sensor ;
- $\mathbf{P}_1$, $\mathbf{P}_2$: Gaussian kernel (size $q = 9$), downsampling (ratio $d = 4$) (Wald, 1997) ;

$\rightarrow$ Compute $\mathcal{Y}_H$ and $\mathcal{Y}_M$, white Gaussian noise with 25dB SNR ;

- Comparison : matrix + tensor CP approaches ;
- Reconstruction metrics : CC, SAD, ERGAS,

$$\text{R-SNR} = 10\log_{10}\left(\frac{\|\mathcal{Y}\|_F^2}{\|\widehat{\mathcal{Y}} - \mathcal{Y}\|_F^2}\right).$$

Reconstruction performance

Pavia University : $\mathcal{Y} \in \mathbb{R}^{608 \times 366 \times 103}$.

Algorithm	R-SNR	CC	SAD	ERGAS	Time
CNMF	21.0696	0.98098	4.7999	3.1572	41.489
GLP-HS	19.1725	0.97056	5.5144	3.7771	49.4237
HySure	20.6336	0.97359	5.7032	3.3481	114.8173
STEREO	**22.0935**	**0.98142**	**4.4306**	**2.7245**	12.5444
SCOTT	21.1754	0.97769	4.4578	2.9826	**0.95689**
Blind-STEREO	21.9284	0.98073	4.5495	2.753	15.2409
BSCOTT	**22.7449**	**0.98382**	**4.3375**	**2.5519**	**0.64972**

- Reconstruction : **SCOTT** < STEREO ;
- Computation time : **SCOTT** $\ll$ STEREO.

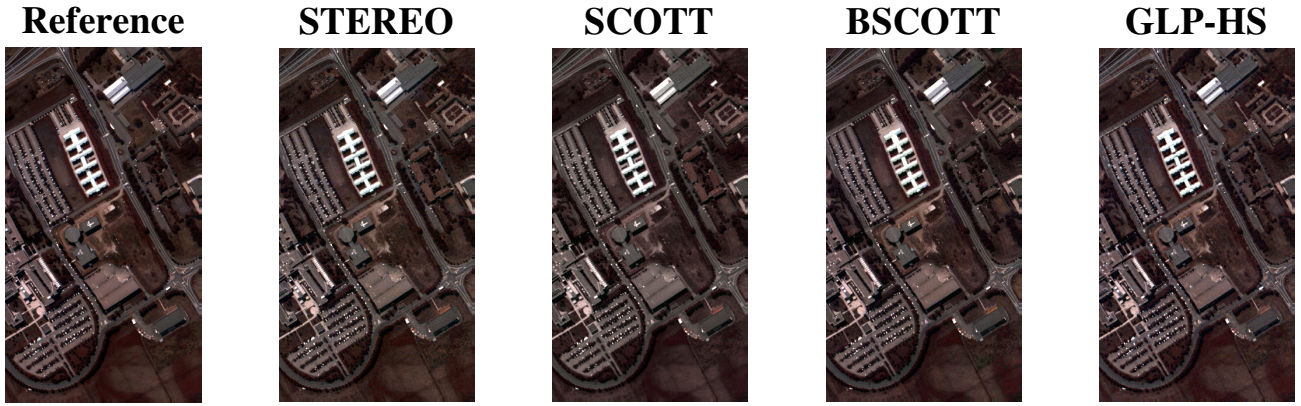

BTD-based HSR with image variability

Inter-image variability

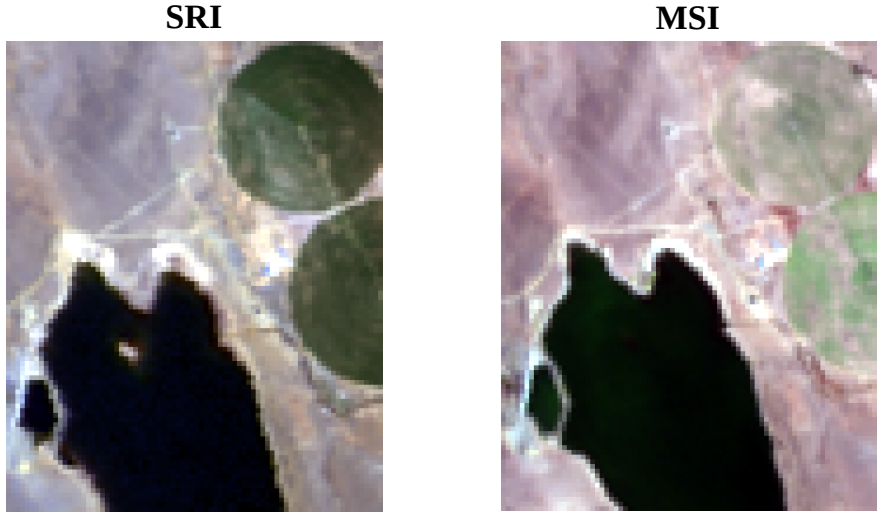

Images acquired by different satellites or at different dates lead to :

- Different atmospheric conditions
- Illumination variations
- Seasonal changes

The acquired images can be subjected to inter-image variability.

A more flexible coupling model

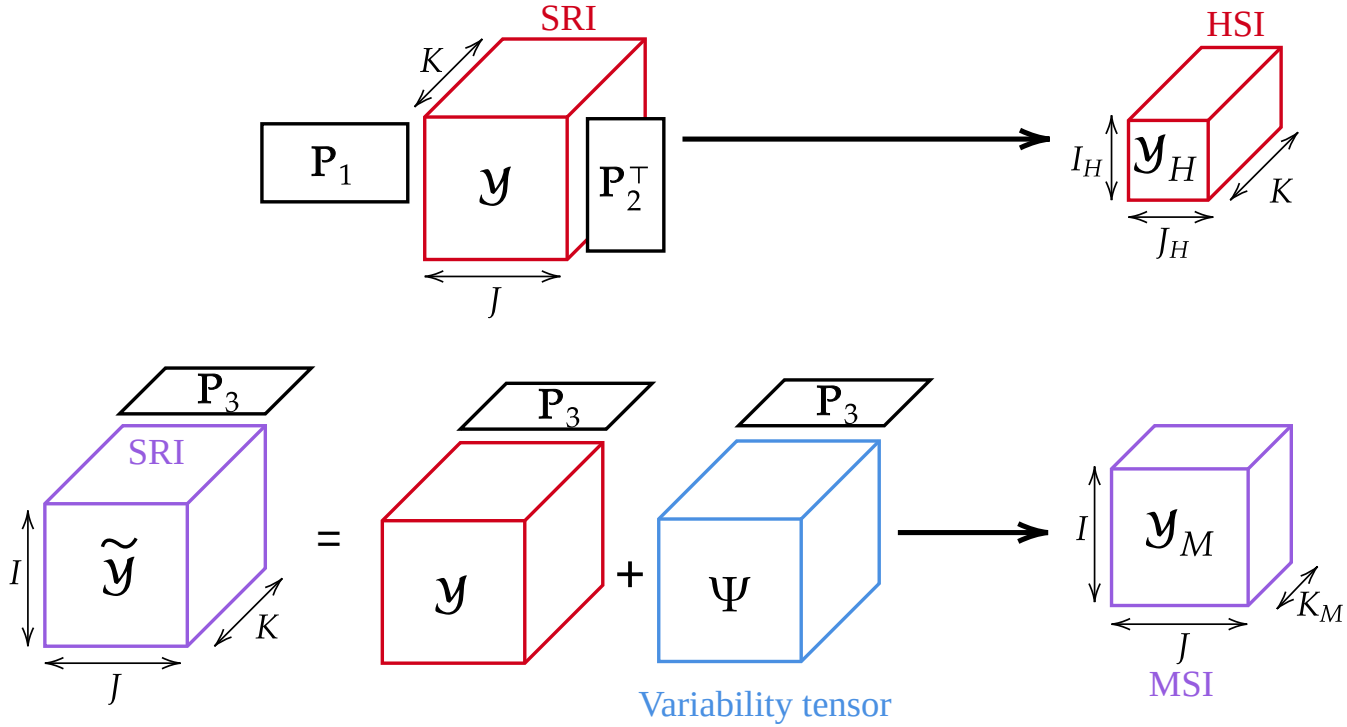

$$\begin{cases} \mathcal{Y}_H &= \mathcal{Y} \bullet_1 \mathbf{P}_1 \bullet_2 \mathbf{P}_2 + \mathcal{E}_H, \\ \mathcal{Y}_M &= \tilde{\mathcal{Y}} \bullet_3 \mathbf{P}_3 + \mathcal{E}_M = (\mathcal{Y} + \Psi) \bullet_3 \mathbf{P}_3 + \mathcal{E}_M. \end{cases}$$

BTD for fusing images with inter-image variability

Model

Assuming a Tucker model for the HRI and variability tensor :

$$\mathcal{Y} = [[\mathcal{G}_Y; \mathbf{U}_Y, \mathbf{V}_Y, \mathbf{W}_Y]], \qquad \mathbf{\Psi} = [[\mathcal{G}_\Psi; \mathbf{U}_\Psi, \mathbf{V}_\Psi, \mathbf{W}_\Psi]],$$

find $\mathcal{Y}$ and $\mathbf{\Psi}$ which satisfies the following model :

$$\begin{aligned}
\mathcal{Y}_H &\approx [[\mathcal{G}_Y; \mathbf{P}_1\mathbf{U}_Y, \mathbf{P}_2\mathbf{V}_Y, \mathbf{W}_Y]], \\
\mathcal{Y}_M &\approx [[\mathcal{G}_Y; \mathbf{U}_Y, \mathbf{V}_Y, \mathbf{P}_3\mathbf{W}_Y]] + [[\mathcal{G}_\Psi; \mathbf{U}_\Psi, \mathbf{V}_\Psi, \mathbf{P}_3\mathbf{W}_\Psi]] \\
&= \sum_{\pi \in \{Y, \Psi\}} [[\mathcal{G}_\pi; \mathbf{U}_\pi, \mathbf{V}_\pi, \mathbf{P}_3\mathbf{W}_\pi]].
\end{aligned}$$

CB-STAR : An optimization-based algorithm

$$\underset{\mathcal{G}_\pi,\mathbf{U}_\pi,\mathbf{V}_\pi,\mathbf{W}_\pi,\pi\in\{Y,\Psi\}}{\text{minimize}} \quad J = \left\| \mathcal{Y}_H - [[\mathcal{G}_Y;\mathbf{P}_1\mathbf{U}_Y,\mathbf{P}_2\mathbf{V}_Y,\mathbf{W}_Y]] \right\|_F^2 + \lambda \left\| \mathcal{Y}_M - \sum_{\pi\in\{Y,\Psi\}} [[\mathcal{G}_\pi;\mathbf{U}_\pi,\mathbf{V}_\pi,\mathbf{P}_3\mathbf{W}_\pi]] \right\|_F^2,$$

BCD strategy

Until stopping criterion is satisfied,

1. Minimize J with respect $\mathcal{G}_Y$ while keeping the others fixed
2. Minimize J with respect $\mathbf{U}_Y$ while keeping the others fixed

$\vdots$

$\widehat{\mathcal{Y}} = [[\widehat{\mathcal{G}}_Y;\widehat{\mathbf{U}}_Y,\widehat{\mathbf{V}}_Y,\widehat{\mathbf{W}}_Y]]$

– Exact recovery conditions
– Computationally demanding

Linear mixing model and LL1

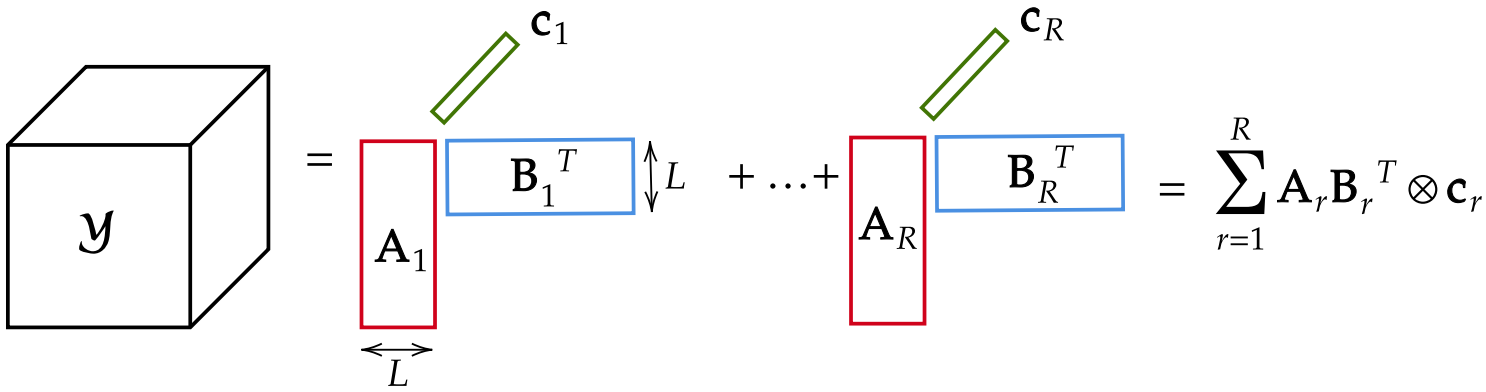

LL1-BTD as linear mixing model

$$\mathcal{Y} = \sum_{r=1}^{R} \mathbf{A}_r \mathbf{B}_r^{\mathsf{T}} \otimes \mathbf{c}_r = \sum_{r=1}^{R} \mathbf{S}_r \otimes \mathbf{c}_r \quad \Leftrightarrow \quad \mathbf{Y}^{(3)} = \mathbf{S}\mathbf{C}^{\mathsf{T}},$$

- $\mathbf{c}_r$: spectral signatures,
- $\mathbf{S}_r$: abundance maps with **low-rank** L : $\mathbf{S}_r = \mathbf{A}_r \mathbf{B}_r^{\mathsf{T}}$;

⚠ Non-negative factors (interpretability).

Spectral variability

Simple model

$$\widetilde{\mathbf{C}} = \psi + \mathbf{C},$$

ψ : spectral variability factor ;

Less general variability than CB-STAR but **less restrictive** recovery conditions.

$$\mathcal{Y} = \sum_{r=1}^{R} \mathbf{A}_r \mathbf{B}_r^\top \otimes \mathbf{c}_r, \quad \Psi = \sum_{r=1}^{R} \mathbf{A}_r \mathbf{B}_r^\top \otimes \psi_r,$$

$$\widetilde{\mathcal{Y}} = \sum_{r=1}^{R} \mathbf{A}_r \mathbf{B}_r^\top \otimes \widetilde{\mathbf{c}}_r = \sum_{r=1}^{R} \mathbf{A}_r \mathbf{B}_r^\top \otimes (\mathbf{c}_r + \psi_r).$$

Super-resolution and blind unmixing

Partial coupling and non-negativity

$$\underset{\mathbf{A},\mathbf{B},\mathbf{C},\widetilde{\mathbf{C}}}{\text{minimize}}\ \mathcal{J} = \left\| \mathcal{Y}_H - \sum_{r=1}^{R} (\mathbf{P}_1 \mathbf{A}_r (\mathbf{P}_2 \mathbf{B}_r)^\mathsf{T}) \otimes \mathbf{c}_r \right\|_F^2 + \lambda \left\| \mathcal{Y}_M - \sum_{r=1}^{R} (\mathbf{A}_r \mathbf{B}_r^\mathsf{T}) \otimes \widetilde{\mathbf{c}}_r \right\|_F^2$$
$$\text{s. to } \{\mathbf{S}_r = \mathbf{A}_r \mathbf{B}_r^\mathsf{T}\}_{r=1}^{R} \geq \mathbf{0}, \mathbf{C} \geq \mathbf{0}, \widetilde{\mathbf{C}} \geq \mathbf{0}.$$

CNN-BTD-Var

Until *stopping criterion* is met,

1. Normalize columns of $\mathbf{C}, \widetilde{\mathbf{C}}_M$ with unit norm ;
2. $\mathbf{A}, \mathbf{B}, \mathbf{C}, \widetilde{\mathbf{C}}_M =$ minimize $\mathcal{J}$ (ADMM procedure + non-negativity) ;
3. $\mathbf{S} =$ ADMM procedure : low-rank + non-negativity ;

$\mathbf{Y}^{(3)} = \mathbf{S}\mathbf{C}^\mathsf{T}$, $\Psi \bullet_3 \mathbf{P}_3 = \mathcal{Y}_M - \mathcal{Y} \bullet_3 \mathbf{P}_3$.

HSR + blind unmixing of $\mathcal{Y}$.

Exact recovery

The SRI $\mathcal{Y}$ and degraded SRI $\widetilde{\mathcal{Y}} \bullet_3 \mathbf{P}_3$ are uniquely recovered by

$$\mathcal{Y} = \sum_{r=1}^{R} (\mathbf{A}_r \mathbf{B}_r^\mathsf{T}) \otimes \mathbf{c}_r, \quad \widetilde{\mathcal{Y}} \bullet_3 \mathbf{P}_3 = \sum_{r=1}^{R} (\mathbf{A}_r \mathbf{B}_r^\mathsf{T}) \bullet_3 \mathbf{P}_3 \widetilde{\mathbf{c}}_r,$$

if $I_H J_H \geq LR$, $IJ \geq L^2 R$ and

$$\min\left(\left\lfloor \frac{I}{L} \right\rfloor, R\right) + \min\left(\left\lfloor \frac{J}{L} \right\rfloor, R\right) + \min(K_M, R) \geq 2R + 2.$$

- Only $\Psi \bullet_3 \mathbf{P}_3$ can be recover ;
- $\mathbf{C}$, $\mathbf{P}_3 \widetilde{\mathbf{C}}$, $\mathbf{S}$: unique up to permutation and scaling ;
- Blind unmixing identifiability comes for free.

Fusion setup

- real SRI $\mathcal{Y}$ (AVIRIS) and MSI $\mathcal{Y}_M$ (Sentinel 2-A) ;
  $\mathcal{Y} \to \mathcal{Y}_H$ (decimation factor $d = 4$, filter with unit variance) ;
- $\mathcal{E}_H$ and $\mathcal{E}_M$: white Gaussian noise, 30dB SNR ;
- comparison to matrix and tensor methods .

- **Dataset** : Lockwood, acquired on 2018-08-20 (SRI) and 2018-10-19 (MSI) ; $\mathcal{Y} \in \mathbb{R}^{80 \times 100 \times 173}$.

SRI

MSI

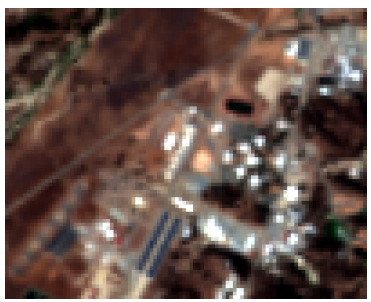

.

Fusion performance

Algorithm	R-SNR	CC	SAM	ERGAS	Time
CNMF	18.7829	0.89063	**2.9768**	6.7014	4.353
HySure	14.125	0.8633	4.4044	11.6	6.9823
STEREO	6.552	0.80196	27.3623	25.1749	**1.8835**
SCOTT	2.2276	0.79276	28.5771	45.9608	**0.2228**
BTD-Var	**20.1273**	**0.918432**	**2.92921**	**6.35566**	5.46272
CNN-BTD-Var	**19.4882**	**0.906525**	3.0299	**6.29101**	4.11573
CB-STAR	19.0751	0.89445	3.3707	7.2926	68.0282

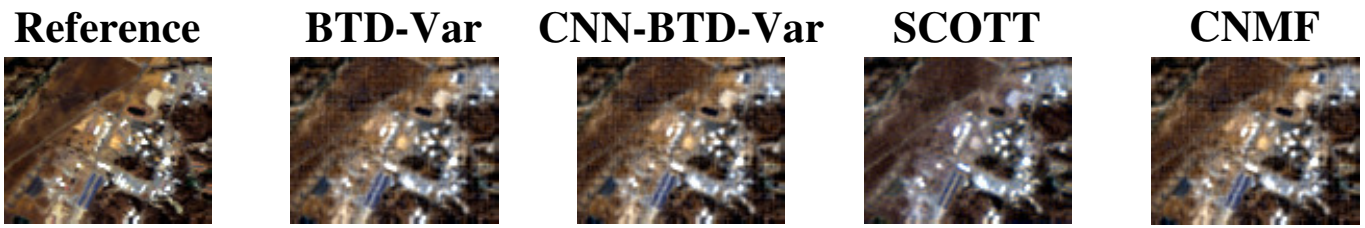

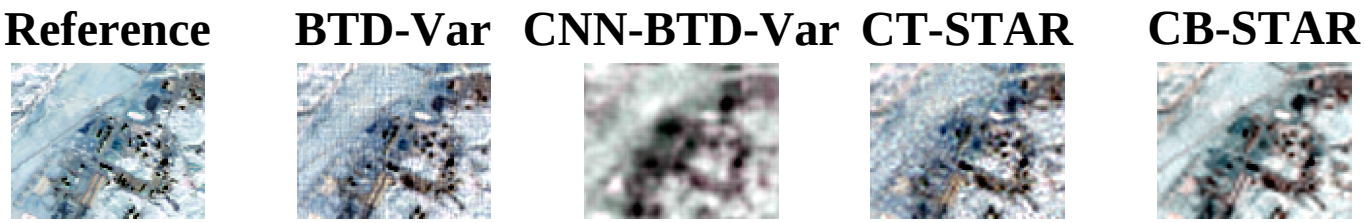

Unmixing setup

- Matrix approach : CNMF (Yokoya et al., 2012) ;
- Two-step procedures :
  CB-STAR + MU-Acc (Gillis et al., 2012), BMDR-ADMM (Nus et al., 2018).
- Lake Tahoe : Acquired on 2014-10-04 (SRI) and 2017-10-24 (MSI) ;
  $\mathcal{Y} \in \mathbb{R}^{80 \times 100 \times 173}$.

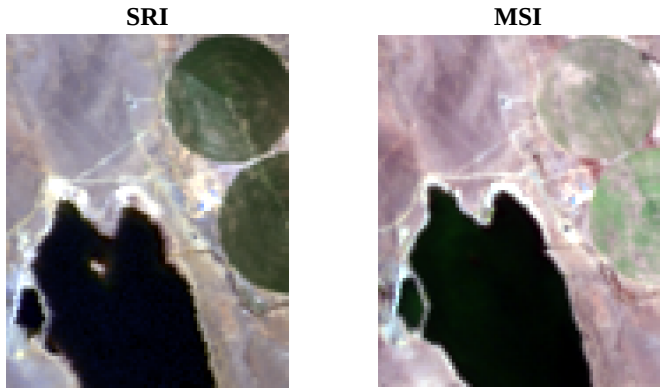

Unmixing performance

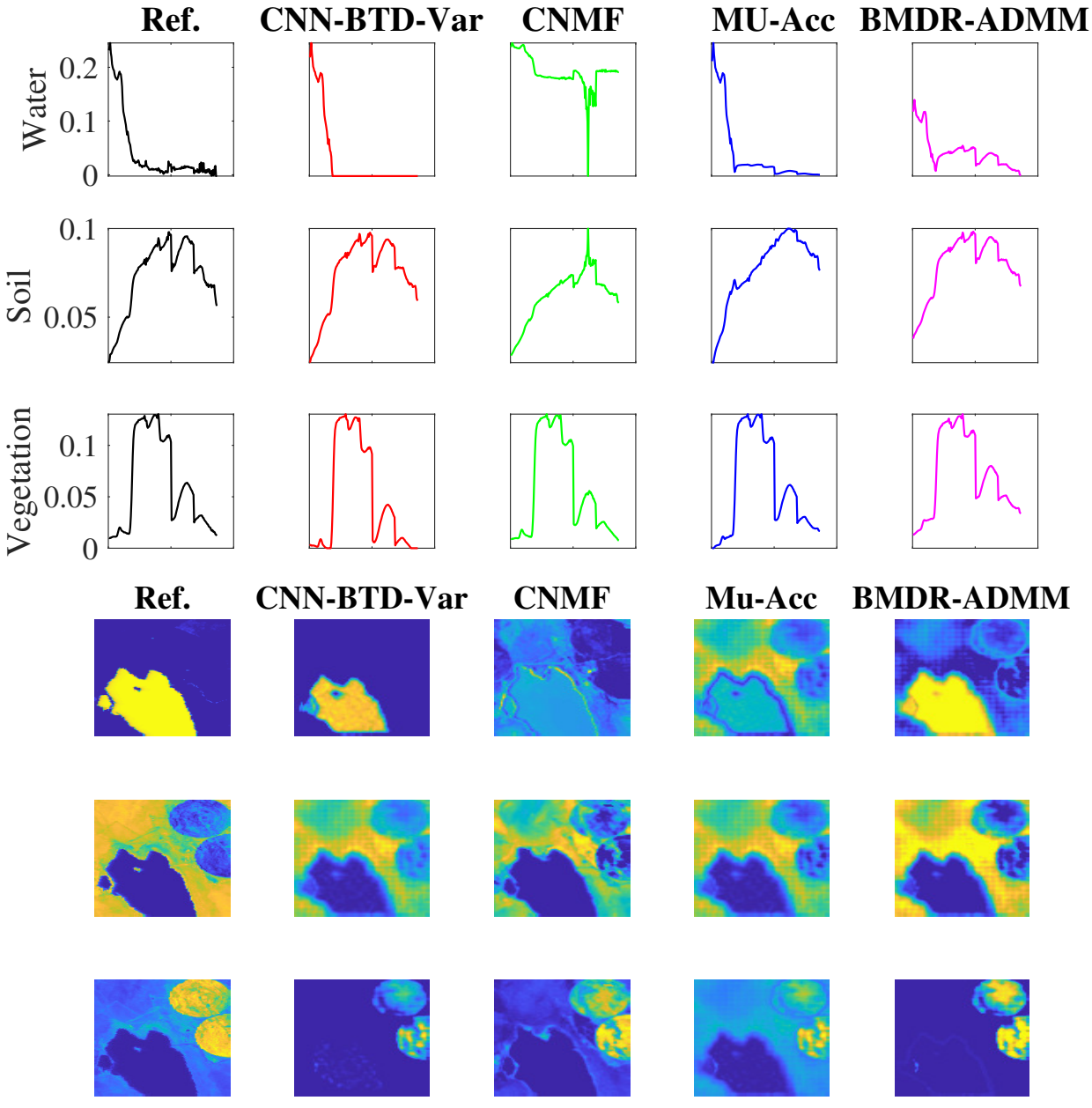

Retrieving the variability factor

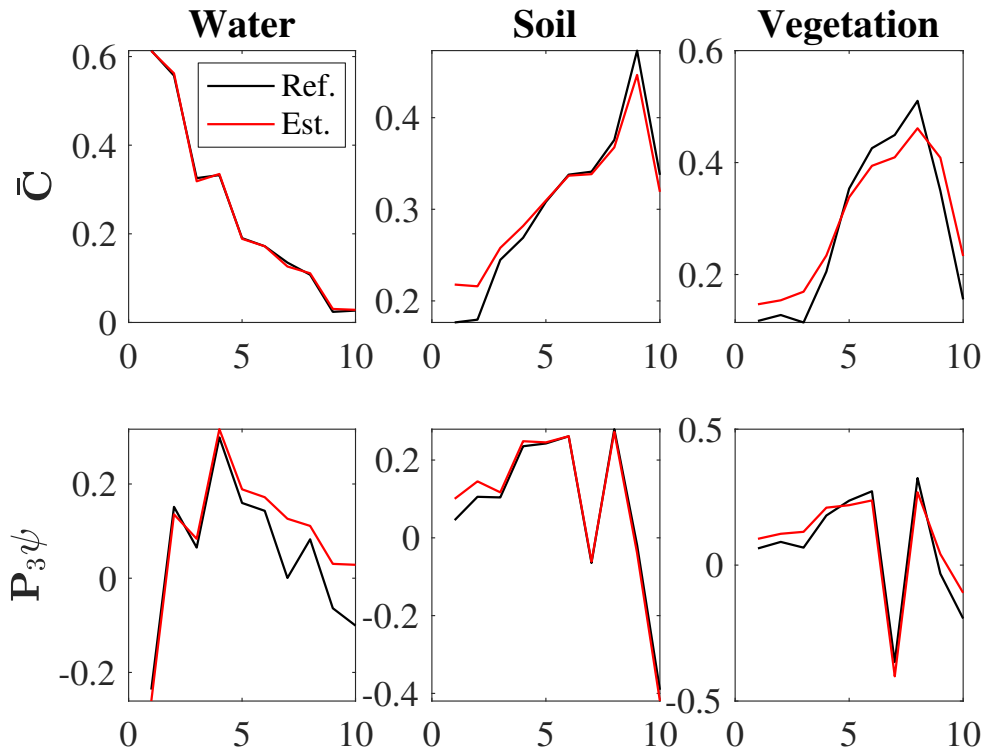

- Water→4th band→ blue wavelengths ;
- Soil→10th band→ orange to infrared wavelengths ;
- Vegetation→7th band→ green wavelengths.

Performance bounds for coupled tensor models

Deriving bounds for coupled tensor models

1. Choose **parameters** : low-rank factors ? Reconstructed tensor ?
2. Identify the **constraints** ;
3. Apply formula according to **scenario** : uncoupled, partially-coupled, fully-coupled ;
4. Evaluate **performance of estimator**.

Bounds

→ Standard CCRB for coupled CP model : performance of STEREO and Blind-STEREO ;
→ Randomly-constrained CRB : application to coupled LL1 models with random variability.

General coupled model

Assumption : Model identifiable.

$$\begin{cases} \mathcal{Y}_1 \sim \mathbf{f}_{\mathcal{Y}_1;\omega} \text{ and } \mathcal{Y}_2 \sim \mathbf{f}_{\mathcal{Y}_2;\omega}, \\ \mathbf{g}(\omega) = \mathbf{0}. \end{cases}$$

Constrained Cramér-Rao bound (CCRB)

$$\mathbf{CCRB}(\omega) = \mathbf{U}\left[\mathbf{U}^{\mathsf{T}}\mathbf{F}\mathbf{U}\right]^{-1}\mathbf{U}^{\mathsf{T}}, \text{ with } \mathbf{U} \text{ a basis of } \ker(\mathbf{G}).$$

Performance of STEREO and Blind-STEREO

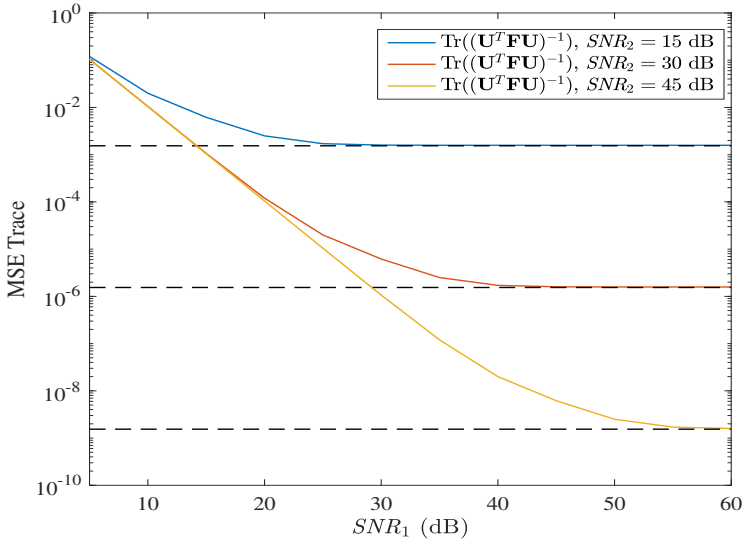

UCCRB versus SNR_1 for different SNR_2.

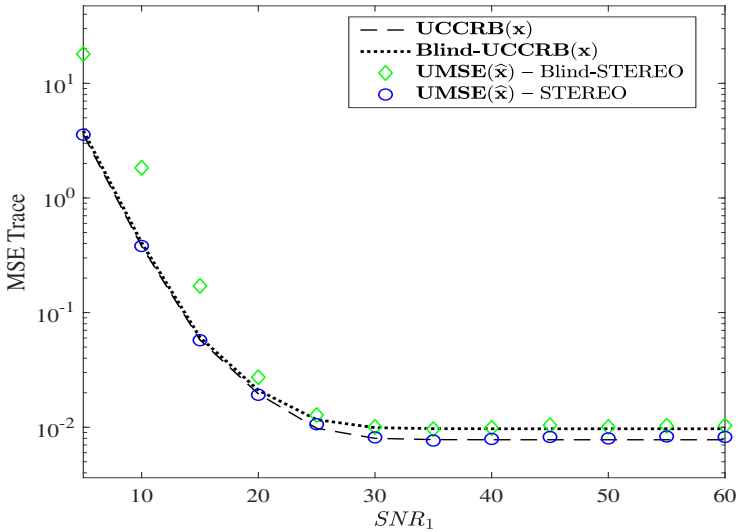

UCCRB and Blind-UCCRB, UMSE from STEREO and Blind-STEREO for $\mathbf{x}$, versus SNR_1 for fixed SNR_2.

Randomly constrained CRB (RCCRB)

- CCRB non-informative when $\mathbf{g}(\omega)$ depends on a random parameter ;
- random parameter θ_r.
- $\widehat{\omega} \triangleq \widehat{\omega}(\mathbf{y})$: locally unbiased cond. to $\boldsymbol{\theta}_r$;

Conditional CCRB

$$\mathbf{CCRB}_{\boldsymbol{\theta}_r}(\omega) = \mathbf{U}_{\boldsymbol{\theta}_r}(\omega)\left(\mathbf{U}_{\boldsymbol{\theta}_r}^T(\omega)\,\mathbf{CRB}_{\boldsymbol{\theta}_r}^{-1}(\omega)\,\mathbf{U}_{\boldsymbol{\theta}_r}(\omega)\right)^{-1}\mathbf{U}_{\boldsymbol{\theta}_r}^T(\omega).$$

RCCRB

$$\mathbf{RCCRB}(\omega) = E_{\boldsymbol{\theta}_r;\omega}\left[\mathbf{CCRB}_{\boldsymbol{\theta}_r}(\omega)\right],$$
$$E_{\mathbf{y}|\omega}\left[(\widehat{\omega}-\omega)(\widehat{\omega}-\omega)^T\right] \geq \mathbf{RCCRB}(\omega).$$

Performance of BTD-Var

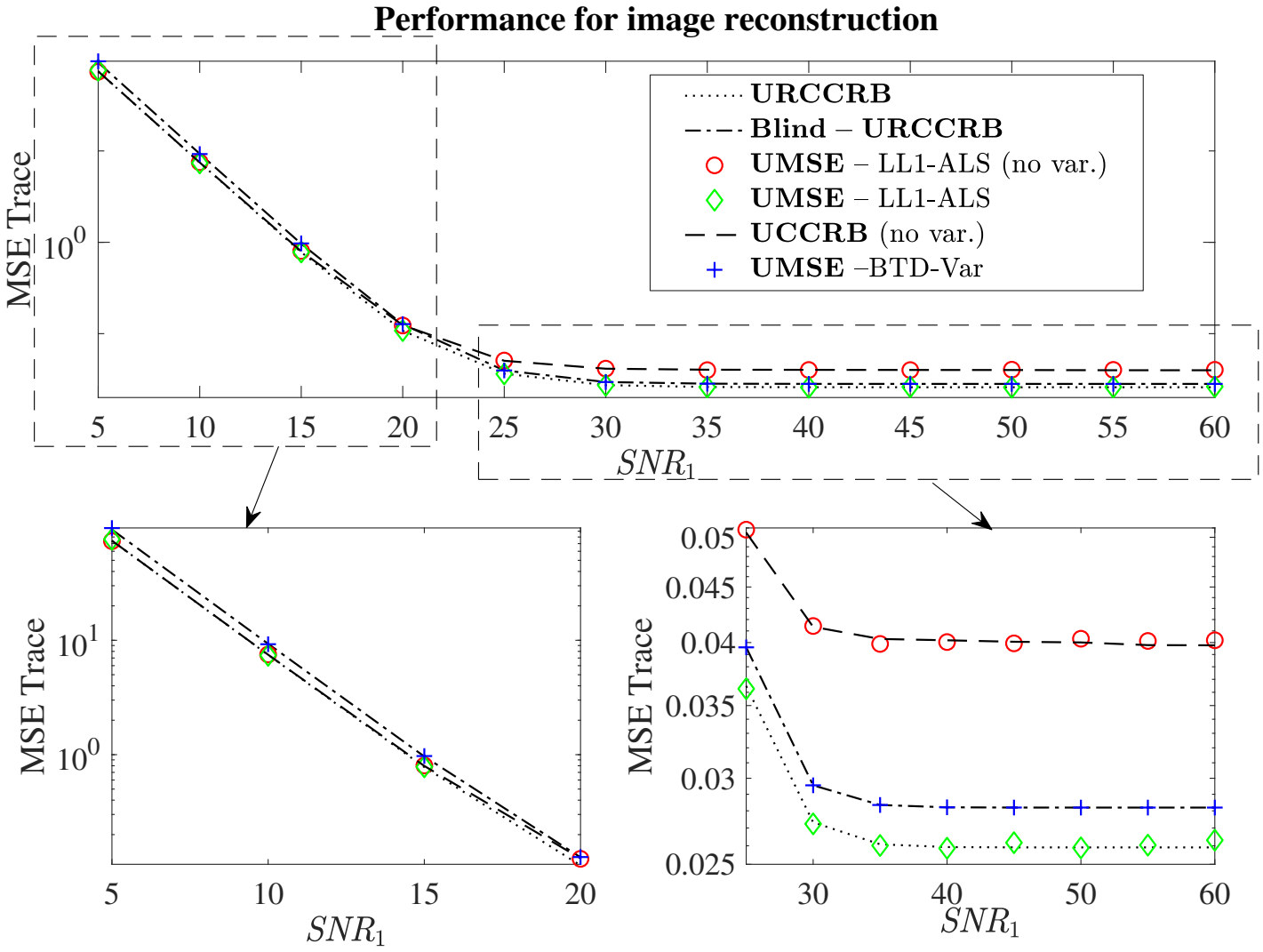

Conclusions

Tensor-based HSR

- Efficient algorithms with exact reconstruction guarantees
- Tensor-based HSR outperforms Matrix based HSR
- HSR without variability
  Performance SCOTT $<$ {STEREO, BTD-LL1}
  Computation time SCOTT $\ll$ STEREO $<$ BTD-LL1
- HSR with variability
  Performance {CT-STAR, CNN-BTD-Var, BTD-Var} $<$ CB-STAR
  Computation time CT-STAR $\ll$ BTD-Var $<$ CNN-BTD-Var $<$ CB-STAR

On-going works

- Coupled CP tensor decomposition with shared and distinct components
- High dimension pdf estimation